Neuron, Vol. 22, 73–87, January, 1999, Copyright ©1999 by Cell Press

Voltage Sensors in Domains III and IV, but Not I and II, Are Immobilized by Na^+ Channel Fast Inactivation

Albert Cha,* Peter C. Ruben,† Alfred L. George, Jr.,‡ Esther Fujimoto,† and Francisco Bezanilla*§

*Departments of Physiology
and Anesthesiology
University of California
School of Medicine
Los Angeles, California 90095

†Department of Biology
Utah State University
Logan, Utah 84322

‡Department of Nephrology
Vanderbilt University
School of Medicine
Nashville, Tennessee 37232

Summary

Using site-directed fluorescent labeling, we examined conformational changes in the S4 segment of each domain of the human skeletal muscle sodium channel (hSkM1). The fluorescence signals from S4 segments in domains I and II follow activation and are unaffected as fast inactivation settles. In contrast, the fluorescence signals from S4 segments in domains III and IV show kinetic components during activation and deactivation that correlate with fast inactivation and charge immobilization. These results indicate that in hSkM1, the S4 segments in domains III and IV are responsible for voltage-sensitive conformational changes linked to fast inactivation and are immobilized by fast inactivation, while the S4 segments in domains I and II are unaffected by fast inactivation.

Introduction

The currents that pass through voltage-gated sodium channels play a critical role in the generation and propagation of action potentials (Hodgkin and Huxley, 1952). Subsequent measurements of the sodium channel gating currents, which arise from the movement of charged residues within the channel in response to voltage, described the voltage dependence and inactivation properties of sodium channels in the squid giant axon (Armstrong and Bezanilla, 1973, 1977). With the advent of molecular biology and the cloning of voltage-gated sodium channels, the molecular components of the sodium channel were elucidated (Noda et al., 1984). The α subunit of the voltage-gated sodium channel contains four domains, each of which contains six transmembrane regions and is homologous to a single subunit of a voltage-gated potassium channel (Noda et al., 1986; Tempel et al., 1987). Each domain (I through IV) contains a number of positively charged, highly conserved amino acids in the fourth transmembrane segment, or S4 segment (Noda et al., 1984; Greenblatt et al., 1985; Kosower, 1985). The S4 segment has been shown to be important in the voltage dependence of channel opening (Stühmer et al., 1989; Shao and Papazian, 1993; Perozo et al., 1994). Studies of charge per channel have demonstrated that several basic residues in the S4 segment play an important role as part of the voltage sensor for voltage-gated ion channels (Aggarwal and MacKinnon, 1996; Seoh et al., 1996).

Fast inactivation of sodium currents is an important mechanism for reducing the influx of sodium into the cell during the generation of the action potential. The relationship between gating charge movement and fast inactivation was first described in the squid giant axon (Armstrong and Bezanilla, 1977). The sodium channel gating charge became immobilized at depolarizing potentials in a voltage- and time-dependent manner coinciding with fast inactivation, and the percentage of charge immobilized by fast inactivation constituted approximately two-thirds of the total gating charge. After the sequence and putative topology of the sodium channel were determined, many studies examined the motifs that are important for fast inactivation of the sodium channel. Unlike potassium channels, which are composed of four identical subunits, the four domains of the sodium channel and the linkers between the domains have distinct functions. For instance, the linker between domains III and IV contains three residues that are critical for fast inactivation (Vassilev et al., 1988; Stühmer et al., 1989; West et al., 1992). This channel asymmetry leads one to the question of whether S4 segments in particular domains may be immobilized by fast inactivation to differing degrees.

Recent studies have used site-directed mutagenesis and chemical modification in various regions of the sodium channel in order to determine what roles specific domains may play in the structure and function of the channel. Mutations in all domains have effects on fast inactivation (Chahine et al., 1994; McPhee et al., 1994, 1995, 1998; Chen et al., 1996; Kontis and Goldin, 1997). However, mutations in the domain IV S4 segment appear to have a preferential and dramatic effect on fast inactivation (Chahine et al., 1994; Chen et al., 1996), and both the S4–S5 loop and the S6 segment in domain IV appear to be involved in fast inactivation (McPhee et al., 1994, 1995, 1998). In comparison, the effects of mutations on other domains have differential effects on inactivation and activation as well. For instance, although the charge neutralizations in domain III do not appear to have an effect on the time constants of fast inactivation, the steady state inactivation and peak activation curves are substantially affected (Chen et al., 1996). In domain II, mutations in different residues suggest that some residues may be involved in activation (Mitrovic et al., 1998), while other residues may be involved in activation and inactivation (Kontis and Goldin, 1997).

It is clear that mutations in different domains have differential effects on activation, deactivation, and inactivation. However, part of the problem in inferring functional roles for specific domains from these mutations is that the mutation may affect more than one function

§ To whom correspondence should be addressed: (e-mail: fbezanil@ucla.edu).

of the channel, either through interactions with other domains or through functional coupling of different regions. For instance, mutations that affect activation may also affect inactivation, because inactivation is coupled to activation. This work addresses these concerns by using site-directed fluorescent labeling to examine domain-specific conformational changes in the human skeletal muscle sodium channel hSkM1. This approach has been successfully used to examine conformational changes in specific regions of the *Shaker* potassium channel (Mannuzzu et al., 1996; Cha and Bezanilla, 1997, 1998). Because this sodium channel does not contain any extracellularly modifiable cysteines or intrinsic fluorescence signals (see Experimental Procedures), we examined conformational changes in the S4 segment of each domain by substituting cysteine for residues in each domain's S4 segment, covalently attaching the extrinsic fluorescent probe tetramethylrhodamine maleimide (TMRM) and examining fluorescence changes as a function of voltage. The kinetics of these fluorescence changes are highly specific for each domain and reveal that the S4 segments in domains III and IV are coupled to fast inactivation, whereas the S4 segments in domains I and II are unaffected by fast inactivation. In addition, domains III and IV contain the gating charge that is immobilized by fast inactivation.

Results

Gating Current Properties of the Wild-Type and Mutant hSkM1 Channels

To examine the properties of fast inactivation of hSkM1, we measured ionic and gating currents as a function of time and pulse potential. The gating currents were measured in the absence of ionic currents with the external application of tetrodotoxin (TTX), and examples of the ionic and gating currents are shown in Figure 1A. The ionic currents were obtained by subtracting the gating currents from the initially measured membrane currents. Because the kinetics of hSkM1 gating currents are fast, the electrophysiological recordings were done with the cut open oocyte technique for fast temporal resolution (Stefani et al., 1994). All traces shown in this work were measured with this technique. The voltage dependence of gating current displacement was measured by integrating the gating charge (Q) for a 10 ms pulse and plotting it against the pulse voltage (V) (Figure 1B). In comparison to the peak conductance versus voltage, or G_{peak}–V curve, the Q–V curve is shifted to more hyperpolarized potentials. This indicates that there is a substantial fraction of gating charge displacement that precedes channel opening.

To measure the effects of fast inactivation on gating charge movement, the gating currents during deactivation, or OFF gating currents, were measured as a function of duration and pulse potential (Figure 1C). For a pulse from −110 to −20 mV (top traces), the peak OFF gating current initially increases with longer pulses, reflecting the recruitment of additional gating charge movement with time. In contrast, as fast inactivation develops later, the peak OFF gating current decreases with longer pulses, and the slow component of the OFF gating current predominates. This change is more apparent in pulses to 0 and 30 mV, in which gating charge becomes immobilized after very short pulses. Thus, during deactivation, there is a fast component with a time constant of ~100–200 μs and a slower component with a time constant on the order of 1–2 ms, which becomes the predominant component as fast inactivation develops. The ON charge is always equal to the OFF charge if both fast and slow components are integrated. This slow component reflects the return of gating charge that has been immobilized by fast inactivation, as first reported by Armstrong and Bezanilla (1977). We measured the voltage dependence and kinetics of this gating charge immobilization by integrating the two components separately and plotting the percentage of total charge contained in the slow charge component as a function of pulse duration and potential (Figure 1D). These curves illustrate the time course and voltage dependence of gating charge immobilization, which correlates with the voltage dependence and time course of inactivation. The maximum fraction of total charge immobilized by fast inactivation is ~67%.

To determine which domains are involved in various aspects of fast inactivation, we turned to site-directed fluorescent labeling to examine the effects of fast inactivation on the fluorescence signals in each domain.

Fluorescence Signals in Domain I Show No Component Associated with Fast Inactivation

The serine at residue 216 (S216) and arginine at residue 219 (R219), the latter residue representing the first charged residue in the S4 segment of domain I, were mutated to cysteine in the hSkM1 sodium channel in order to examine conformational changes in this region. For the remainder of the paper, each mutant channel construct will be referenced by the original amino acid followed by its number and "C" for the substituted cysteine (e.g., S216C). Fluorescence signals were measured by attaching TMRM to these sites. The voltage-dependent fluorescence changes at site S216C display very fast kinetics in comparison to the currents during activation and deactivation for a 5 ms pulse (Figures 2A and 2B). In addition, there is no visible component of fluorescence signal with a time course corresponding to fast inactivation, which suggests that movement of the S4 segment in domain I does not appear to undergo conformational changes directly associated with the fast inactivated state. The voltage dependence of the fluorescence change was determined by measuring the change in fluorescence at the end of the 5 ms pulse as a function of pulse potential (Figure 2C). This F–V curve is hyperpolarized in comparison to the Q–V curve, suggesting that this domain undergoes conformational changes at more hyperpolarized potentials than the bulk of the gating charge. The fluorescence signals obtained from site R219C were very similar to those seen at S216C (data not shown).

To examine the effects of fast inactivation on the S4 segment in domain I, the characteristics of the fluorescence signal were examined with depolarizing pulses of varying lengths to either 0 or 50 mV (Figures 2D and

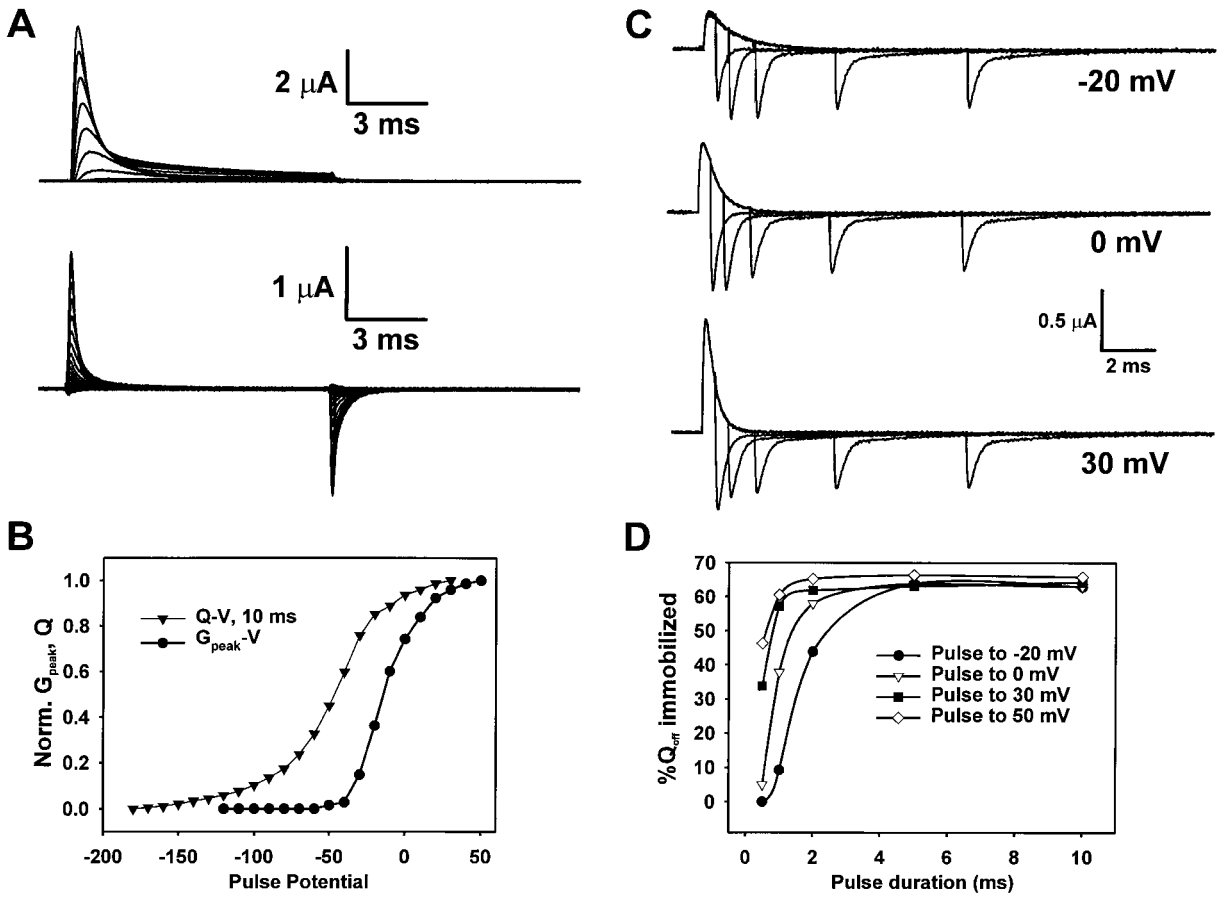

Figure 1. Wild-Type hSkM1 Ionic and Gating Currents

(A) Ionic currents, obtained by subtraction (see Experimental Procedures) (top) and gating currents (bottom, obtained after TTX block) measured from hSkM1 with the cut open oocyte technique. The currents were measured from a holding potential of −90 mV, prepulsed to −130 mV for 10 ms, and then depolarized to potentials from −120 to 40 mV for 10 ms before returning to −130 mV. The traces were obtained with P/-4 at a subtraction potential of −130 mV (ionic) or with P/4 at a subtraction potential of 50 mV (gating). The external and internal solutions contained 120 mM NMG-Mes to minimize sodium currents for better voltage control. The ionic currents consist of outward potassium currents from the remaining potassium within the oocyte.

(B) The voltage dependence of normalized gating charge displacement (Q) and normalized peak ionic currents (G_{peak}) were measured as a function of pulse potential (V). The gating charge was calculated by integrating the gating charge for the traces in (A) and normalizing to the maximum charge displaced.

(C) The time course of immobilization of the OFF gating currents is apparent for pulses from −110 to −20 mV (top traces), 0 mV (middle traces), or 30 mV (bottom traces) for durations of 0.5, 1.0, 2.0, 5.0, and 10.0 ms.

(D) The percentage of total charge contained in the slow charge component was calculated as a function of pulse duration and potential (see Experimental Procedures). The percentage was determined for pulses from −110 to −20 mV (closed circles), 0 mV (open, inverted triangles), 30 mV (closed squares), and 50 mV (open diamonds).

2E). The ionic currents, obtained by subtracting gating currents after TTX block from the initial membrane currents, are shown above the corresponding fluorescence changes, with dotted lines demarcating the end of the depolarizing pulses. By measuring fluorescence deactivation characteristics as a function of pulse duration, the effect of fast inactivation on conformational changes in the domain I S4 segment alone can be carefully examined. If the domain I S4 segment were immobilized by inactivation, one would expect either a large change in the time course of fluorescence deactivation, a large change in the delay before the onset of fluorescence deactivation, or both.

A visual inspection of the fluorescence kinetics during deactivation for different pulse durations to either 0 or 50 mV indicates that the fluorescence deactivation is unaffected by the length of the pulse (Figures 2D and 2E). Thus, fluorescence deactivation appears to be unaffected by the degree of fast inactivation, in comparison to the ionic currents shown above the fluorescence traces. This absence of modulation by pulse duration can be quantitated by measuring the delay in the onset of fluorescence change after the repolarization of membrane potential (Figure 3A). For domain I, the delay is longer than the settling time of the voltage clamp, which is typically <100 μs, but does not change as a function of pulse potential or duration. The fluorescence deactivation kinetics were also measured by fitting a single exponential to the fluorescence trace during repolarization (Figure 3B). These kinetics are subtly affected by

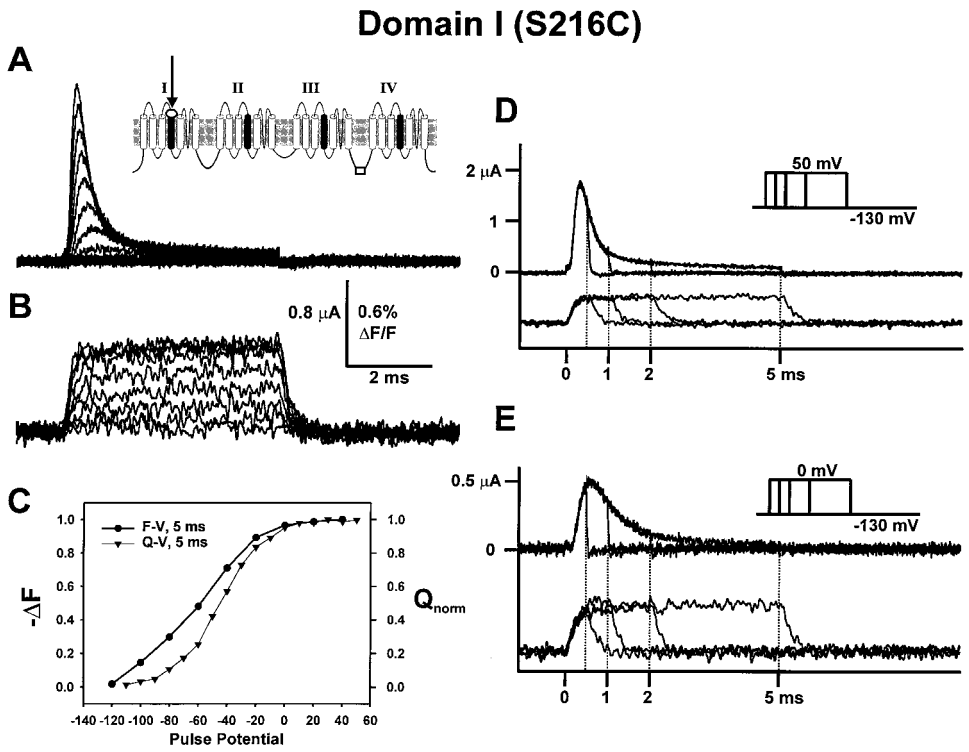

Figure 2. Fluorescence Characteristics of the Domain I S4 Segment

(A) Ionic currents, obtained by subtraction, taken from TMRM-labeled S216C hSkM1 channels from −130 mV to potentials ranging from −120 to 50 mV for 5 ms. (Inset) Schematic which notes that the data in this figure were obtained from domain I.

(B) Changes in fluorescence intensity measured for labeled S216C channels measured from −130 to −100, −80, −60, −40, −20, 0, and 20 mV. The fluorescence traces were taken as averages of 60 sweeps.

(C) The change in fluorescence intensity at the end of the 5 ms pulse (ΔF) and normalized gating charge displacement (Q) were plotted as a function of pulse potential (V). The fluorescence change and gating charge displacement were normalized to their maximum values.

(D) Ionic currents, obtained by subtraction (top), and fluorescence traces (bottom) measured for four different durations in a pulse from -130 to 50 mV for 0.5, 1, 2, and 5 ms. The dotted lines represent the end of the pulse for the different pulse durations. The fluorescence traces were taken as averages of 80–100 sweeps.

(E) Ionic currents, obtained by subtraction (top), and fluorescence traces (bottom) for pulses to 0 mV with a protocol otherwise identical to (D).

pulse duration and amplitude, as the time constant increases from ~150 to 250 μs for a 10 ms depolarization. However, this modulation is not consistent with immobilized charge recovering from inactivation, which has a time course of >1 ms.

Another method for testing the effects of inactivation on fluorescence utilizes a conditioning, depolarizing prepulse that is used to modulate the fraction of the channels in the fast inactivated state (Figure 3C). The fraction of channels available to open was tested after this conditioning prepulse by pulsing from the holding potential to a test potential of 50 mV. The channels were either prepulsed to 0 mV for 2 or 10 ms, or no prepulse was applied. With this protocol, there is a substantial decrease in ionic current during the 50 mV test pulse when the conditioning prepulse is applied, consistent with an increase in the fraction of inactivated channels. However, the fluorescence signal maintains the same magnitude and kinetics during the pulse to 50 mV, without regard to the amount of channel inactivation. This clearly demonstrates that channel inactivation does not affect fluorescence changes in domain I and strongly argues that the domain I S4 segment is not immobilized by fast inactivation. The fluorescence activation kinetics, which are fast, suggest that domain I is not directly coupled to fast inactivation. The deactivation kinetics, which are also fast and are mostly unaffected by fast inactivation, indicate that the S4 segment of domain I is not involved in recovery from fast inactivation.

Fluorescence Signals in Domain II Are Also Unaffected by Fast Inactivation

In domain II, fluorescence signals were measured at sites S666C and R669C, the latter residue representing the first charged residue in the S4 segment. The voltage-dependent fluorescence changes at site S666C displayed very fast kinetics very similar to those seen in domain I (Figure 4B). Again, there is no visible component of fluorescence signal with a time course corresponding to fast inactivation, which suggests that domain II does not undergo conformational changes directly associated with the fast inactivated state. The voltage dependence of the F–V curve is also shifted to hyperpolarized potentials in comparison to the Q–V curve, consistent with gating charge in domain II also moving at more hyperpolarized potentials than the main component of the gating charge. The fluorescence signals obtained from site R669C were very similar to those seen at site S666C (data not shown).

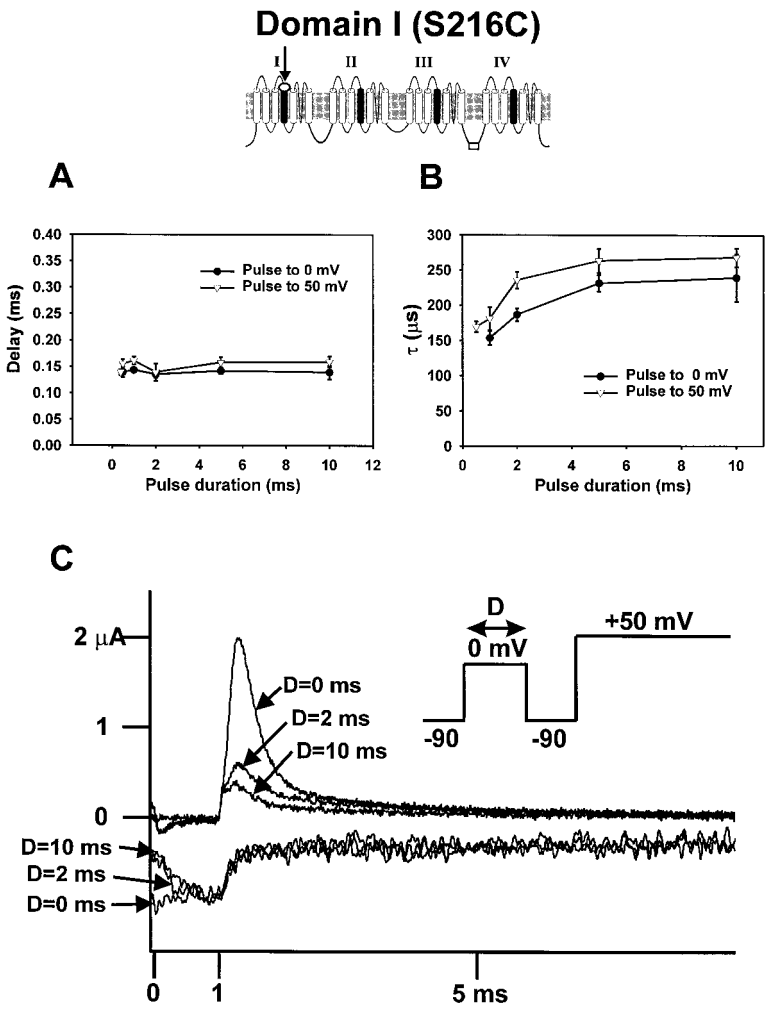

Figure 3. Fast Inactivation Characteristics of the Domain I S4 Segment

(Top) Schematic which notes that the data in this figure were obtained from domain I.

(A) Delay in fluorescence deactivation after the end of the depolarizing pulse as a function of pulse potential (0 mV, closed circles; 50 mV, open triangles) and duration. Error bars indicate standard error of the mean (SEM) (n = 5).

(B) Kinetics of fluorescence deactivation as a function of pulse potential, with symbols identical to (A).

(C) Triple pulse protocol with varying conditioning prepulses to 0 mV from a holding potential of −90 mV, followed by a 1 ms repolarization to -90 mV and a test pulse to 50 mV. Membrane current traces (top, mostly ionic) correspond to no prepulse (D = 0 ms), a 2 ms prepulse (D = 2 ms), or a 10 ms prepulse (D = 10 ms). The fluorescence traces (bottom) correspond to a 10 ms prepulse (D = 10 ms), a 2 ms prepulse (D = 2 ms), or no prepulse (D = 0 ms). The fluorescence traces were taken as averages of 100 sweeps.

The effects of inactivation on the S4 segment in domain II were examined with a variable length depolarizing pulse to either 0 or 50 mV (Figures 4D and 4E). An inspection of the fluorescence kinetics during deactivation for different pulse durations indicates that the fluorescence deactivation is unaffected by the length of the pulse. Thus, as in domain I, fluorescence deactivation appears to be unaffected by the degree of inactivation. This independence of deactivation kinetics from pulse duration was quantified by measuring both the delay before the onset of fluorescence change (Figure 5A) and the fluorescence deactivation kinetics (Figure 5B). Neither the delay nor the deactivation kinetics were affected by pulse duration or potential, consistent with the domain II S4 segment moving independently of fast inactivation.

Using a conditioning prepulse to place a variable fraction of the channels in the fast inactivated state before a test pulse, the ionic currents reveal a substantial increase in channel inactivation with a prepulse to 0 mV (Figure 5C). However, the fluorescence signal maintains the same magnitude and kinetics during the test pulse to 50 mV, showing no effect from the extent of channel inactivation. As in domain I, this clearly demonstrates that the level of channel inactivation does not affect fluorescence changes in domain II and strongly argues that the domain II S4 segment is not immobilized by fast inactivation. The fluorescence activation kinetics, which are monotonic and fast, suggest that domain II is not directly coupled to fast inactivation. The deactivation kinetics, which are very fast and unaffected by fast inactivation, indicate that domain II is uninvolved in recovery from fast inactivation.

Fluorescence Signals in Domain III Correlate with Fast Inactivation and with Charge Immobilization

Domain III fluorescence signals were measured at site K1126C, which represents the first charge in the S4 segment. The voltage-dependent fluorescence changes at site K1126C display slower kinetics than those seen in domains I and II (Figure 6B). In addition, for large depolarizations, there is a second, slower fluorescence component that is more clearly seen in the fluorescence traces in Figure 6B or in the traces in Figure 6D. This slow fluorescence component moves in the opposite direction of fluorescence activation and is responsible for the decrease in fluorescence change seen in the F–V curve (Figure 6C). This slow component can also be seen in the fluorescence deactivation for long pulses to

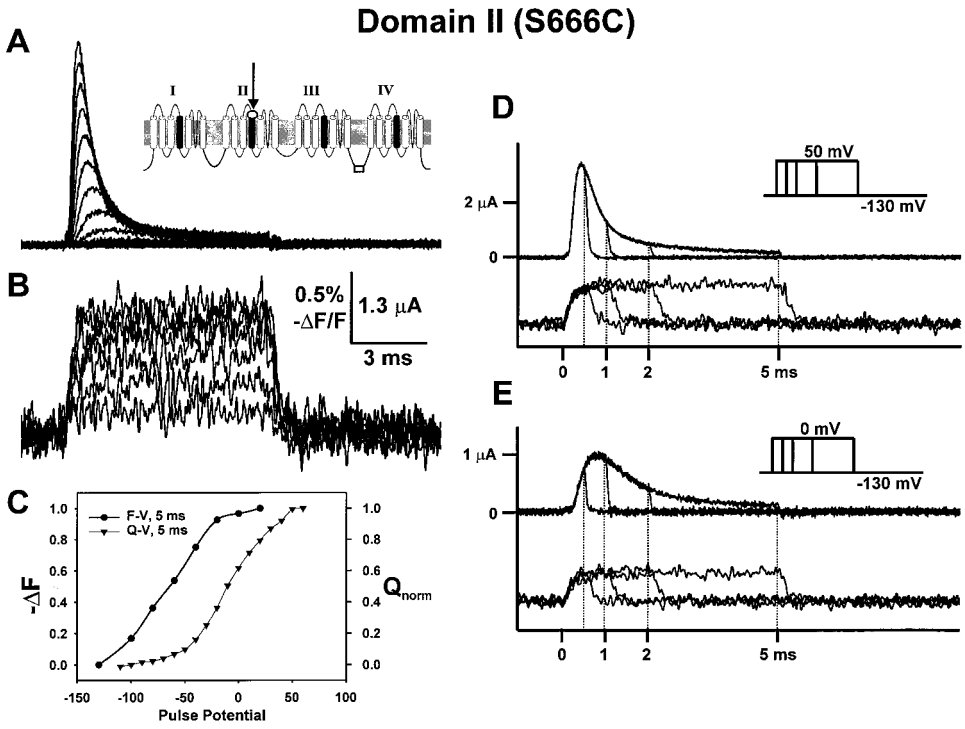

Figure 4. Fluorescence Characteristics of the Domain II S4 Segment

(A) Ionic currents, obtained by subtraction, taken from TMRM-labeled S666C hSkM1 channels from −130 mV to potentials ranging from −120 to 50 mV for 5 ms. (Inset) Schematic which notes that the data in this figure were obtained from domain II.

(B) Changes in fluorescence intensity measured for labeled S666C channels from −130 to −100, −80, −60, −40, −20, 0, and 20 mV. The fluorescence traces were taken as averages of 100 sweeps.

(C) The change in fluorescence intensity at the end of the 5 ms pulse (ΔF) and gating charge displacement (Q) were plotted as a function of pulse potential (V).

(D) Ionic currents, obtained by subtraction (top), and fluorescence traces (bottom) measured for four different durations in a pulse from -130 to 50 mV for 0.5, 1, 2, and 5 ms. The dotted lines represent the end of the pulse for the different pulse durations. The fluorescence traces were taken as averages of 100 sweeps.

(E) Ionic currents, obtained by subtraction (top), and fluorescence traces (bottom) for pulses to 0 mV with a protocol otherwise identical to (D).

large depolarizations, whereby the fluorescence actually undershoots the initial intensity level before returning to the initial state (Figure 6B and Figure 6D, inset). These fluorescence changes may reflect slow conformational changes associated with the onset of and recovery from fast inactivation and are not seen in domains I or II.

The effects of inactivation on the S4 segment in domain III were examined with a variable length depolarizing pulse to either 0 or 50 mV (Figures 6D and 6E). By examining the fast component of fluorescence deactivation for different pulse durations to 50 mV, in contrast to domains I and II, the fluorescence deactivation is significantly affected by the length of the pulse. In particular, the delay before the onset of fluorescence deactivation becomes prolonged, with a time course and voltage dependence similar to ionic inactivation (Figure 7A). This result indicates that domain III is likely immobilized by fast inactivation. In contrast, the fluorescence deactivation kinetics after this delay do not change with pulse duration (Figure 7B). This implies that there is a deactivation step in domain III, whose rate is not dependent upon the level of fast inactivation, and this step occurs only after a delay that follows the time course of fast inactivation.

The fluorescence signal is also greatly affected by the conditioning prepulse (Figure 7C). The fluorescence change associated with activation is seen only when no prepulse is applied and essentially disappears when a 0 mV prepulse of either 2 or 10 ms is applied to the channels. This is clearly different from the results seen in domains I and II and argues that the domain III S4 segment is immobilized by fast inactivation. The slow component of fluorescence kinetics during activation and deactivation suggests that domain III also undergoes conformational changes associated with fast inactivation.

Fluorescence Changes in Domain IV Show Kinetics that Correlate with Fast Inactivation Kinetics

Fluorescence signals were examined in domain IV at site R1448C, which represents the first charge in the S4 segment. The fluorescence signals demonstrate two components: a fast component, which is seen for depolarizations of 1 ms or less, and a slow component, which forms the predominant component of the fluorescence and is more readily visible during long depolarizations (Figure 8B). The fluorescence changes were examined for a 40 ms pulse, during which the slow component is clearly visible, and the fluorescence kinetics are as slow

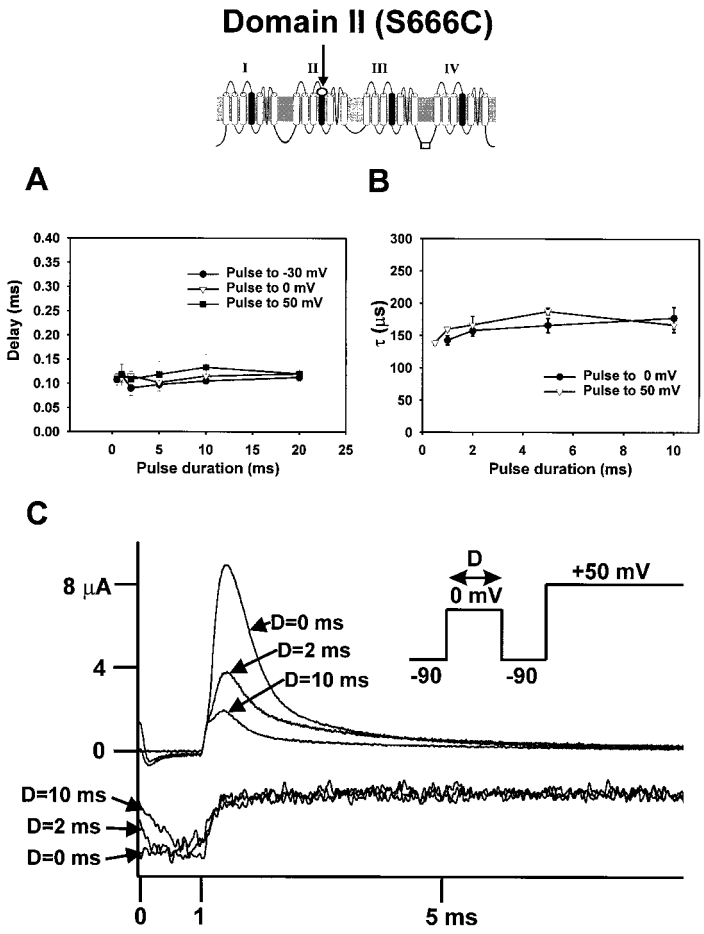

Figure 5. Fast Inactivation Characteristics of the Domain II S4 Segment

(Top) Schematic which notes that the data in this figure were obtained from domain II.

(A) Delay in fluorescence deactivation after the end of the depolarizing pulse as a function of pulse potential (-30 mV, open circles; 0 mV, open triangles; 50 mV, closed squares) and duration. Error bars = SEM (n = 4).

(B) Kinetics of fluorescence deactivation as a function of pulse potential (0 mV, closed circles; 50 mV, open triangles). Error bars = SEM (n = 4).

(C) Triple pulse protocol with varying conditioning prepulses to 0 mV from a holding potential of −90 mV, followed by a 1 ms repolarization to -90 mV and a test pulse to 50 mV. Membrane current traces (top, mostly ionic) correspond to no prepulse (D = 0 ms), a 2 ms prepulse (D = 2 ms), or a 10 ms prepulse (D = 10 ms). The fluorescence traces (bottom) correspond to a 10 ms prepulse (D = 10 ms), a 2 ms prepulse (D = 2 ms), or no prepulse (D = 0 ms). The fluorescence traces were taken as averages of 80 sweeps.

or slower than the time course of fast inactivation (Figures 8A and 8B). In contrast to the other domains, the F–V curve is shifted to more depolarized potentials than the Q–V curve (Figure 8C). Although slower than fast inactivation, this slow component of the fluorescence may represent conformational changes into and from the fast inactivated state.

Using a variable duration depolarization and examining the kinetics of fluorescence deactivation, it is clear that for short depolarizations, the fluorescence deactivates relatively quickly but deactivates very slowly for longer depolarizations (Figures 8D and 8E). This implies that the conformational change in the domain IV S4 segment may contain two components: one associated with activation of the channel and another corresponding to a transition into the immobilized, fast inactivated state. The effect of inactivation on fluorescence deactivation is clearly seen by plotting the time constant of fluorescence return as a function of pulse potential and duration (Figure 9A). The time constant becomes as slow as 8 ms for long depolarizations but is much faster for short depolarizations, consistent with an effect that correlates with fast inactivation. Although these fluorescence time constants appear much slower than those seen for fast inactivation of the wild-type channel, the domain IV channel also inactivates three to five times more slowly than the wild-type channel (Table 1).

The fluorescence change in domain IV is also heavily modulated by a conditioning prepulse that modulates the level of inactivation. The fluorescence change in a test pulse to 50 mV is hardly visible when a prepulse to 50 mV is applied, in comparison to the fluorescence change measured without prepulse (Figure 9B). This experiment also strongly argues that fast inactivation immobilizes the S4 segment in domain IV.

Discussion

Gating currents from hSkM1 show the same general features of the gating currents recorded from the squid axon sodium channel. There is a large fraction of the charge that moves in the negative region of membrane potential, where no conduction is observed, and it exhibits voltage- and time-dependent charge immobilization that follows the inactivation of the conductance (Figure 1). These observations appear to be generic to voltage-dependent sodium channels, which allows us to use them as the basis for correlating the function with the structure of the channel. The labeling of specific sites of the channel with fluorescent probes has allowed us to go one step further in associating the different aspects of the channel function with specific structural domains.

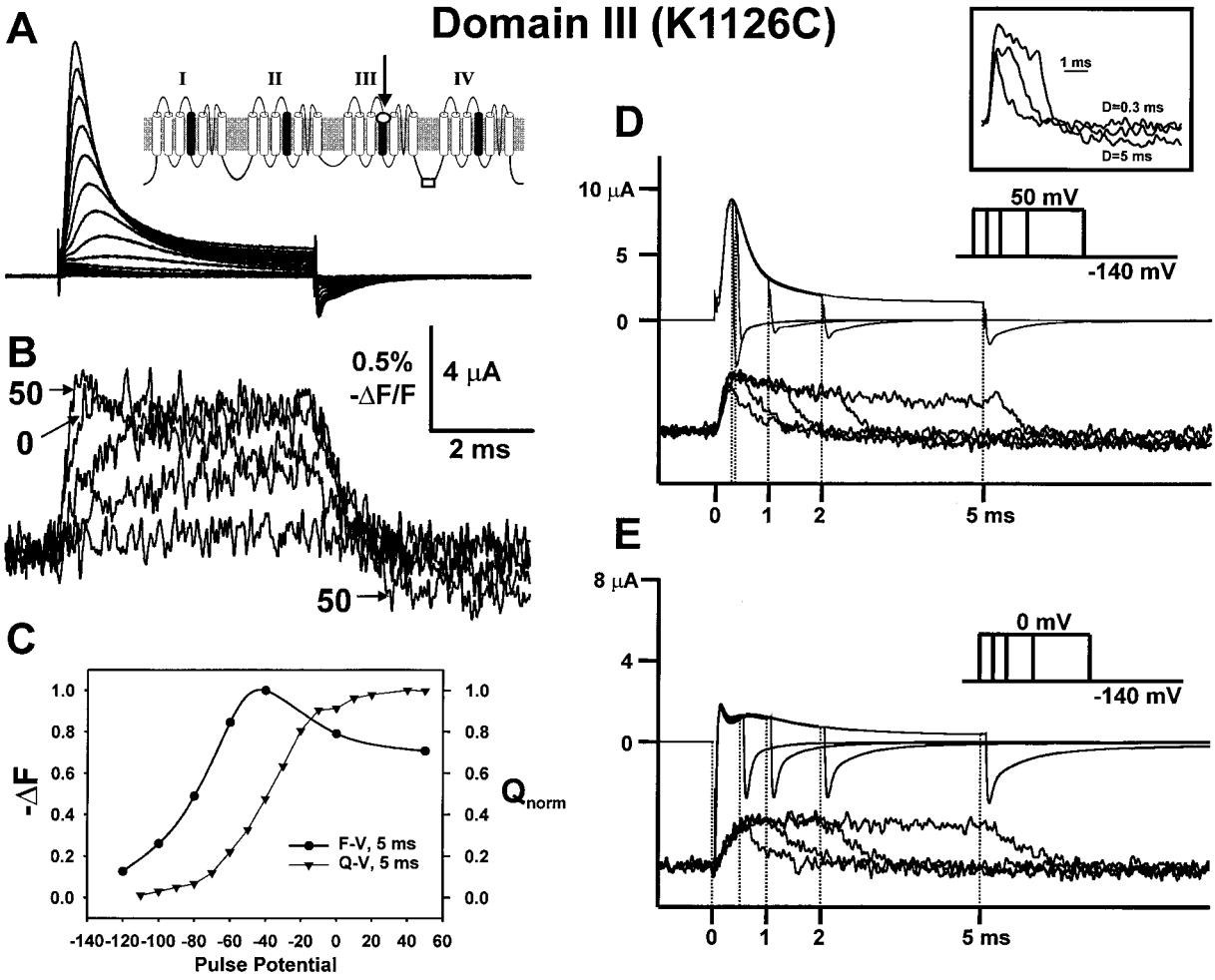

Figure 6. Fluorescence Characteristics of the Domain III S4 Segment

(A) Membrane currents (mostly ionic) taken from TMRM-labeled K1126C hSkM1 channels from −140 mV to potentials ranging from −120 to 50 mV for 5 ms. The tail currents are primarily gating currents. (Inset) Schematic which notes that the data in this figure were obtained from domain III.

(B) Changes in fluorescence intensity measured for labeled K1126C channels measured from −140 to −80, −60, −40, 0, and 50 mV. The arrows designate pulses to 0 and 50 mV (trace with undershoot). The fluorescence traces were taken as averages of 80 sweeps.

(C) The change in fluorescence intensity at the end of the 5 ms pulse (ΔF) and gating charge displacement were plotted as a function of pulse potential (V).

(D) Membrane currents (top, mostly ionic) and fluorescence traces (bottom) measured for five different durations in a pulse from −140 to 50 mV for 0.4, 0.5, 1, 2, and 5 ms. The dotted lines represent the end of the pulse for the different pulse durations. The fluorescence traces were taken as averages of 100 sweeps. (Inset) Fluorescence changes following pulses from −140 to 50 mV for durations of 0.3 ms, 2 ms, and 5 ms. The largest undershoot during repolarization is seen after the 5 ms pulse, with no undershoot seen during repolarization after the 0.3 ms pulse. Traces were filtered to 2 kHz.

(E) Membrane currents (top, ionic and gating) and fluorescence traces (bottom) for pulses from −140 to 0 mV for 0.5, 1, 2, and 5 ms.

Fluorescence Allows the Monitoring of Sites in Specific Domains

Site-directed fluorescent labeling provides a very sensitive measure of the kinetics and voltage dependence of conformational changes at a specific site within a protein. Determining the accessibility of a particular residue to a thiol-reactive compound has also been used in the past to measure conformational changes in specific regions of voltage-gated ion channels (Yang and Horn, 1994; Larsson et al., 1996; Liu et al., 1996; Baker et al., 1998). However, this technique has two limitations. First, it cannot be used to assay conformational changes at sites where there are no changes in accessibility, because nearby protein or lipid interfaces are not restrictive to methanethiosulfonate- (MTS-) based molecules. Thus, the absence of a change in accessibility to MTS-based compounds does not rule out the possibility of conformational changes at that site. In addition, the kinetics of conformational change at these sites are difficult to measure with accessibility studies because of the limited time resolution of applying thiol-reactive compounds. For these reasons, using fluorescence to follow the kinetics and voltage dependence of site-specific conformational changes has definite advantages.

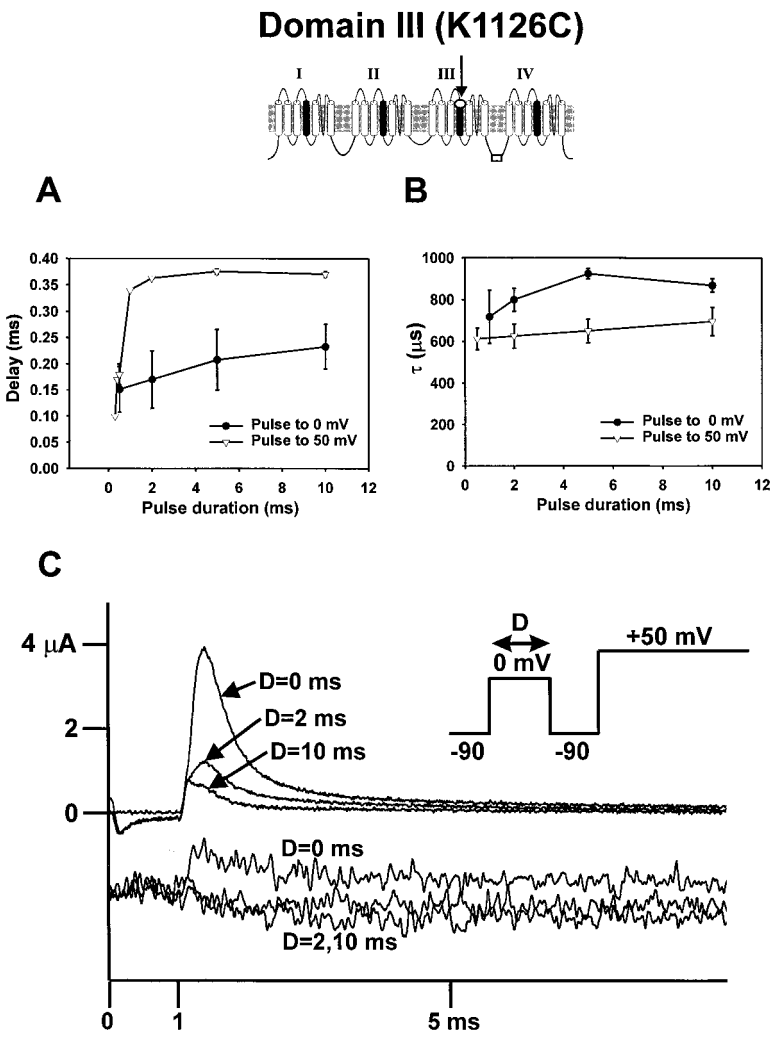

Figure 7. Fast Inactivation Characteristics of the Domain III S4 Segment

(Top) Schematic which notes that the data in this figure were obtained from domain III.

(A) Delay in fluorescence deactivation after the end of the depolarizing pulse as a function of pulse potential (0 mV, closed circles; 50 mV, open triangles) and duration. Error bars = SEM (n = 3).

(B) Kinetics of fluorescence deactivation as a function of pulse potential with symbols identical to (A) (n = 4).

(C) Triple pulse protocol with varying conditioning prepulses to 0 mV from a holding potential of −90 mV, followed by a 1 ms repolarization to -90 mV and a test pulse to 50 mV. Membrane current traces (top, mostly ionic) correspond to no prepulse (D = 0 ms), a 2 ms prepulse (D = 2 ms), or a 10 ms prepulse (D = 10 ms). The fluorescence traces (bottom) correspond to no prepulse (D = 0 ms) or to a 2 or 10 ms prepulse (D = 2 or 10 ms). The fluorescence traces were taken as averages of 100 sweeps.

It can be argued that the cysteine mutation or the fluorescent probe attached to the S4 segment may perturb the function that is under study. Although this is a concern that can be addressed by examining the characteristics of the ionic currents of these channels (Table 1), we are comparing the ionic currents of the labeled, mutated channels directly with fluorescence changes from the same population of channels. As long as the channel still inactivates, we can still determine whether fluorescence in that construct tracks the time course of inactivation. Only the domain IV mutant showed substantial kinetic differences from the wild-type channel, but the channel still undergoes fast inactivation, and the time course of this modified inactivation can be used to interpret the time course of fluorescence changes.

In this study, we have measured fluorescence changes from the inactivating sodium channel. It is reasonable to assume that inactivation is affecting the observed signals and that a noninactivating sodium channel may have a different fluorescence response. In fact, the signals obtained from very short depolarizations mostly reflect the activation, with little contamination from the inactivation process. There is a striking contrast between the deactivation process and the inactivation process, as seen from fluorescence signals in domains III and IV. For very short pulses (500 μs to 50 mV, 1 ms to 0 mV), it is clear that the fluorescence deactivation occurs quickly and without delay in domains III and IV; this likely reflects the normal deactivation of the S4 segments in domains III and IV. During longer depolarizations, the lengthening delay and slower kinetics most likely reflect the immobilization of gating charge by fast inactivation in these domains. A more detailed account of activation alone could be obtained by measuring the fluorescence from noninactivating mutants.

Comparisons of Fluorescence Results to Previous Studies

By examining changes in the intensity of tetramethylrhodamine attached to specific sites, domain-specific involvement of the S4 segment in fast inactivation can be determined. Although previous studies have addressed these roles by mutating residues in different domains, these mutations can have wide-ranging effects that can affect activation, fast inactivation, slow inactivation, and coupling between these functions. It is true that mutations in domains I and II have been shown to have effects on fast inactivation (Chen et al., 1996; Kontis and Goldin, 1997; Kontis et al., 1997). However, it is possible that

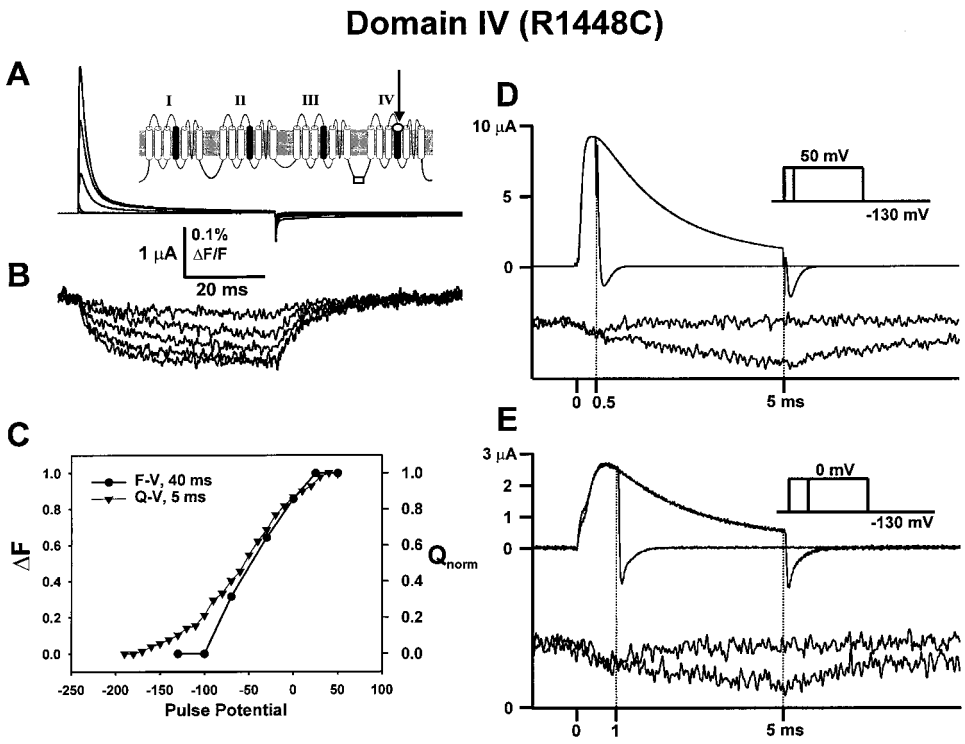

Figure 8. Fluorescence Characteristics of the Domain IV S4 Segment

(A) Membrane currents (mostly ionic) taken from TMRM-labeled R1448C hSkM1 channels from −130 to −70, −30, 0, 25, and 50 mV for 40 ms. (Inset) Schematic which notes that the data in this figure were obtained from domain IV.

(B) Changes in fluorescence intensity measured for labeled R1448C channels with the protocol used in (A). The fluorescence traces were taken as averages of 100 sweeps.

(C) The change in fluorescence intensity at the end of the 5 ms pulse (ΔF) and gating charge displacement (Q) were plotted as a function of pulse potential (V).

(D) Membrane currents (top, ionic and gating) and fluorescence traces (bottom) measured for a 0.5 ms and a 5 ms pulse from −130 to 50 mV. The dotted lines represent the end of the pulse for the different pulse durations. The fluorescence traces were taken as averages of 500 sweeps.

(E) Membrane currents (top, ionic and gating) and fluorescence traces (bottom) measured for a 1 ms and a 5 ms pulse from −130 to 0 mV. The fluorescence traces were taken as averages of 600 sweeps.

mutations in domains that may have only one primary function can also have effects on other related functions. For instance, as activation and inactivation are coupled, mutations that affect activation may also affect inactivation. The most likely explanation for the differences between our data and previous studies is that domains I and II are primarily involved in activation, but mutations in these domains that affect activation also affect inactivation through coupling between activation and inactivation. Another explanation for the difference is that the domains of these channels gate cooperatively, and mutations in one domain may affect the function of neighboring domains. Thus, mutations in domains I and II may indirectly affect the function of domains III and IV.

The involvement of domain IV with fast inactivation measured with fluorescence is consistent with studies that found that mutations in domain IV predominately affect fast inactivation and that the domain IV S4–S5 linker interacts with the isoleucine-phenylalanine-methionine (IFM) motif in the linker between domains III and IV (Chahine et al., 1994; Chen et al., 1996; McPhee et al., 1998). Our data are also consistent with work that found effects on steady state inactivation in domain III (Chen et al., 1996) and interactions between the domain III S4–S5 loop and the IFM motif (Smith and Goldin, 1997). The slow component of fluorescence activation kinetics indicates that domains III and IV undergo slow conformational changes that presage the fast inactivated state.

Developing a Kinetic Model for Fast Inactivation with Identified Domains

Figure 10 summarizes the kinetic steps of sodium channel activation and inactivation in reference to actions of specific domains, based on the results presented in this paper. It is important to note that our results do not allow us to determine a specific sequence of activation during depolarization because of limited time resolution. During activation, if there were a specific sequence that the S4 segments of the different domains followed during depolarization, one would expect variable delays in the fluorescence activation kinetics, with the longest

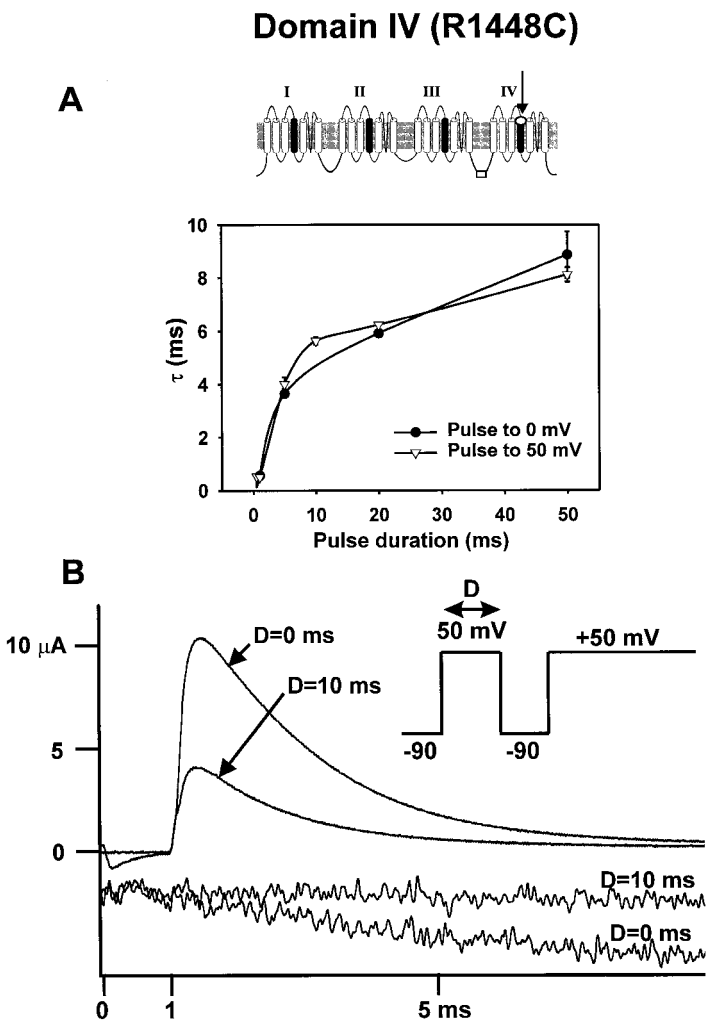

Figure 9. Fast Inactivation Characteristics of the Domain IV S4 Segment

(Top) Schematic which notes that the data in this figure were obtained from domain IV.

(A) Kinetics of fluorescence deactivation after the end of the depolarizing pulse as a function of pulse potential (0 mV, closed circles; 50 mV, open triangles) and duration. Error bars = SEM (n = 5).

(B) Triple pulse protocol with either a 10 ms conditioning prepulse to 50 mV from a holding potential of −90 mV or no prepulse, followed by a 1 ms repolarization to −90 mV and a test pulse to 50 mV. Membrane current traces (top) correspond to no prepulse (D = 0 ms) or a 10 ms prepulse (D = 10 ms). The fluorescence traces (bottom) correspond to no prepulse (D = 0 ms) or to a 10 ms prepulse (D = 10 ms). The fluorescence traces were taken as averages of 500 sweeps.

delay for the S4 segment that moves last. Therefore, only the shaded path of the scheme presented in Figure 10 is supported by the fluorescence data, with the direction indicating the deactivation sequence concomitant with the recovery from inactivation.

Following a depolarization, a sudden repolarization shows that the fluorescence traces in domains I and II return to baseline quickly, and their time course is independent of the duration of the preceding depolarization. After a long depolarization that establishes inactivation, it is unnecessary for the S4 segments in domains III and IV to return to a closed conformation in order for the S4 segments in domains I and II to move. This is represented in Figure 10 as a sequential set of transitions describing the movement of the four domains from the open, fast inactivated state (upper right) to the most closed state (lower left). In this sequence, the domain II S4 segment likely moves first, since it shows the fastest deactivation kinetics (∼150–200 μs) and shortest delay (∼90–130 μs; see Figure 5). The domain I S4 segment follows closely after domain II, with slightly slower deactivation kinetics (∼150–250 μs) and a slightly longer delay than domain II (∼150 μs; see Figure 3).

During recovery from inactivation, the S4 segments

Table 1. Effects of Mutations and Probe Labeling on Ionic Currents of hSkMI Constructs

Construct	$t_{1/2}$ to Peak Current from −130 to 0 mV (μs) (SEM)	$t_{1/2}$ to Peak Current from −130 to 50 mV (μs) (SEM)	τ_{inact} for 5 ms Pulse at 0 mV from −130 mV (μs) (SEM)	τ_{inact} for 5 ms Pulse at 50 mV from −130 mV (μs) (SEM)
Wild-Type	320.42 ± 12.22	186.67 ± 5.11	757.24 ± 46.41	408.07 ± 22.37
S216C	340.00 ± 43.76	218.33 ± 39.75	760.31 ± 115.20	380.77 ± 64.08
S666C	409.00 ± 14.50	229.00 ± 7.93	962.13 ± 118.29	412.93 ± 26.71
K1126C	344.38 ± 20.11	197.63 ± 6.21	843.61 ± 92.21	355.55 ± 35.26
R1448C	425.00 ± 27.25	300.00 ± 23.12	2450.50 ± 197.39	2181.10 ± 218.83

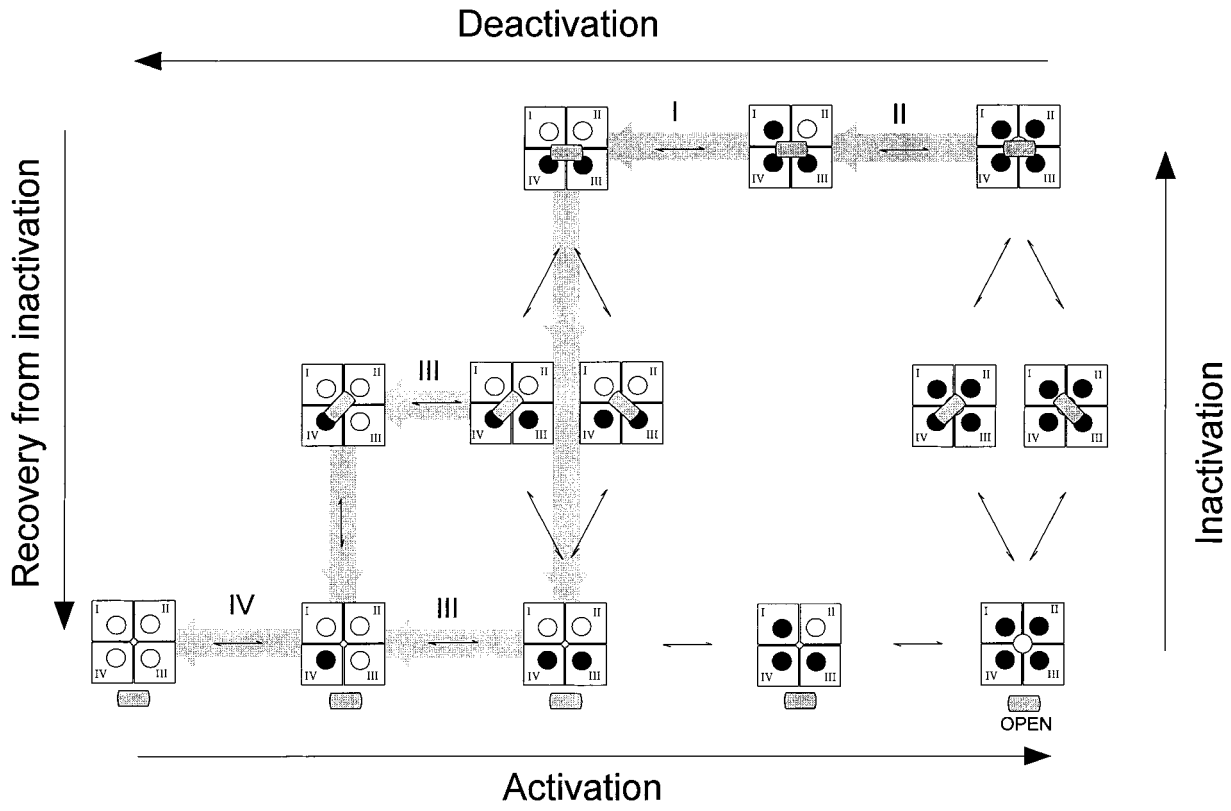

Figure 10. Kinetic Model of Sodium Channel Fast Inactivation

The S4 segments are shown as circles that are open in the resting state and filled in the active state. Domains are labeled from I to IV clockwise, starting from the upper left quadrant of the channel. The inactivation domain is indicated as a small gray bar. Three basic sets of states are shown: upper row, inactivation domain attached to DIII–S4 and DIV–S4 (bar attached to both S4s); middle row, inactivation domain (gray bar) attached to only one of DIII–S4 or DIV–S4; lower row, the inactivation domain (gray bar) is not attached to either domain. The gray arrow indicates the pathway of deactivation and inactivation recovery as can be inferred from the fluorescence results. For details, see text.

of domains III and IV move after the segments of the first two domains. Thus, inactivation immobilizes the S4 segments of domains III and IV but to different extents. The fluorescence signal from domain III still shows relatively fast (~600–900 μs) deactivation kinetics but shows two extra features. There is a slow component (in the opposite direction; see Figure 6) during and after the pulse, and in addition, the deactivation shows a delay that grows with longer depolarizations (see Figures 6 and 7), indicating immobilization by the inactivation domain. In comparison, the S4 segment of domain IV has much slower kinetics (up to 8 ms), but fast inactivation in this construct is also three to five times slower than the other domains (see Table 1). Because the signal to noise in the fluorescence traces is poor in domain IV, it was difficult to determine whether the delay seen during deactivation in domain III was also seen in domain IV.

These observations are modeled in the gray pathway of Figure 10. In this diagram, the inactivation domain interacts with the S4 segments of domains III (DIII–S4) and IV (DIV–S4) but not with the S4 segments of domains I and II. The interaction is represented by attaching the inactivation domain to both DIII–S4 and DIV–S4 together (upper row of states in Figure 10) or separately (middle row of states in Figure 10). This produces two steps in the recovery from inactivation, and to account for the data, we make the lower step (the release of the second contact point of the inactivation domain) rate limiting. DIII–S4 may return to its closed position only after releasing the inactivation domain, but this may occur either while the inactivation domain is still attached to DIV–S4 (fast) or after it has detached from DIV–S4 (slow), giving two components to the return of DIII–S4 fluorescence signal. Notice that DIV–S4 will only return after DIII–S4 has returned and will always be rate limited by the last (slow) detachment of the inactivation domain, giving origin to a slow fluorescence signal. The delay observed in the fluorescence signal of DIII–S4 is represented by the first detachment of the inactivation domain (step between the upper and middle row of states in Figure 10). This single step is expected to produce a delay that is too short compared with the experimental fluorescence trace. A better representation of this delay could be achieved by assuming that the attachment of the inactivation domain occurs with multiple interaction sites, giving origin to a high degree of cooperativity. In this view, the first detachment would occur only after all of these sites are released, introducing a delay before the second step of inactivation recovery may proceed. This delay probably also arises because of the difference

in the return of inactivated as compared with noninactivated channels (see below).

The observed charge immobilization can also be visualized in the scheme of Figure 10. After a pulse that has produced inactivation, most channels would be in the upper rightmost state. Repolarization of the membrane would produce charge movement of domains I and II in very much the same way as the charge that comes back for a short pulse that did not produce inactivation; this is the nonimmobilized gating charge. The charge of domains III and IV will have to wait for the detachment of the inactivation domain, and that constitutes the immobilized charge that returns to its resting position with the time course of recovery from inactivation. The charge of domain IV is completely immobilized by inactivation (lower row), while a fraction of the charge of domain III may return quickly (middle row) or slowly (lower row). The measured immobilization is about 66% of the charge. It would tempting to correlate this quantity with the number of basic residues in the S4 of the different domains. However, as it has been shown that the total charge movement depends on only some of the charges of the S4 segment (Aggarwal and MacKinnon, 1996; Seoh et al., 1996), the correlation becomes questionable until a measurement of charge per channel is done for neutralizations of each of the different domains.

The details of the diagram excluded by the gray arrow pertain to the sequence of activation. There is no reason a priori to think that it must follow the same order of the deactivation sequence in presence of inactivation. For example, before inactivation settles, deactivation may be initiated by DIII–S4 or DIV–S4 (instead of DII–S4 followed by DI–S4), because they are not yet immobilized by the inactivation domain. This scenario would help explain the delay of the fluorescence recovery of domain III, because as the S4 segment would move immediately in noninactivated channels, the delay would be much shorter for short duration pulses than for long duration pulses, when the majority of channels are fast inactivated, and domain III would move after domains I and II. Higher time resolution fluorescence experiments performed at lower temperatures are expected to reveal the details of the activation and deactivation pathways.

The model presented here is similar to many models of inactivation proposed before (Armstrong and Bezanilla, 1977; Armstrong and Gilly, 1979; Horn and Vandenberg, 1984; Stimers et al., 1985; Patlak, 1991; Vandenberg and Bezanilla, 1991; Kuo and Bean, 1994). There are differences, such as the two step process for the remobilization of the charge, that explain the differences between the fluorescence signals of DIII and DIV. Also, the data of this paper do not support models in which immobilization can occur from all states of the activation pathway (Stimers et al., 1985; Kuo and Bean, 1994). It is not yet possible to decide whether the immobilized S4 segments move back quickly after the inactivation particle has dissociated or slowly with the inactivation particle attached. However, regardless of the order of particle dissociation, the most striking difference from previous results is that instead of referring to a generic percent of charge immobilization, we are now able to specify which domains are immobilized by inactivation.

Experimental Procedures

Modified Cut Open Oocyte Epifluorescence Setup

The optical setup has been described before (Cha and Bezanilla, 1998). It consisted of an Olympus BX50WI (Olympus Optical, Melville, NY) and employed excitation filters, dichroic mirrors, and emission filters (Omega Optical, Brattleboro, VT and Chroma Technologies, Brattleboro, VT) appropriate for TMRM (Molecular Probes, Eugene, OR). The microscope objective was a LumPlanFL 40X water immersion objective with a numerical aperture of 0.8 and long working distance of 3.3 mm (Olympus Optical). Light measurements were made with a PIN-020A photodiode (UDT Technologies, Torrance, CA) mounted on an FP-1 fiber optic manipulator (Newport, Irvine, CA), which was attached to the front end of an optical splitter at the microscope's epifluorescence port. Voltage clamp of the oocyte was performed with a CA-1 cut open oocyte clamp (Dagan, Minneapolis, MN). The experimental external solution contained 120 mM NMG-Mes, 10 mM HEPES, and 2 mM $Ca(Mes)_2$ at pH 7.4. The experimental internal solution contained 120 mM NMG-Mes, 10 mM HEPES, and 2 mM EGTA at pH 7.4.

Data Acquisition and Analysis

Gating, ionic, and fluorescence currents were acquired with a PC44 board (Innovative Technologies, Moorpark, CA), which interfaces with a Pentium-based computer via an IBM-compatible AT slot. The fluorescence and electrophysiology were simultaneously acquired on two 16 bit analog-to-digital converters and transferred to two separate channels of the PC44. When data is sampled at intervals longer than 5 μs (all traces presented in this paper), the program running the PC44 board acquires the data at 5 μs per point and then decimates the data to the required sampling period after digitally filtering the original data to the new Nyquist frequency. The acquisition program and data analysis programs were developed in house and were run in MS-DOS and Windows 95, respectively.

The fluorescence delay (Figures 3A, 5A, and 7A) was determined by fitting an exponential to the decay of the fluorescence deactivation, and then measuring the time from the end of the depolarization to the point at which the exponential meets the level of fluorescence during the depolarization.

Subtracted ionic current traces (Figures 1A, 2A, 2D, 2E, 4A, 4D, and 4E) were obtained by subtracting gating currents obtained after TTX block from the previously recorded membrane currents during the same experiment. The tail currents for the unsubtracted membrane currents shown in Figures 6A, 6D, 6E, 8A, 8D, and 8E are primarily made up of gating currents.

The peak G–V curve (Figure 1B) was obtained with an internal solution of 15 mM NaMes and an external solution of 1 mM NaMes (with N-methyl-glucamine (NMG) to replace the remaining cations). The reversal potential was determined from an instantaneous I–V after subtracting the gating component, and peak conductance was calculated by dividing peak current by the voltage difference from the reversal potential. Within the time resolution of the clamp, the instantaneous I–V curve was linear, so no further corrections were made.

The gating charge immobilization (Figure 1D) was computed by fitting a single exponential to the slow component of the OFF gating current, extrapolating the exponential to the beginning of deactivation, subtracting the fitted exponential from the OFF gating current, integrating the remaining fast component of gating current, subtracting the fast charge component from the total gating charge, and dividing by the total gating charge.

Molecular Biology and Channel Expression

The hSkM1 cRNA was transcribed from a pSP64T vector in vitro with SP6 polymerase (Ambion, Austin, TX) after linearization with EcoRI. The β subunit was transcribed from pBluescript in vitro with T7 polymerase (Ambion) after linearization with HindIII. Control mutations were prepared by the PCR overlap extension method of site-directed mutagenesis (Ho et al., 1989). A PCR fragment containing the mutation was ligated into unique sites in the wild-type hSkM1/SP64T cDNA. For S216C, a 1.4 kb SalI–SexAI fragment was prepared; for S666C, a 480 bp SexAI–FseI frament was prepared.

Clones were verified by sequencing. Fifty nanoliters cRNA containing equal volumes of 1 μg/μl α subunit and 3 μg/μl β subunit was injected into each *Xenopus* oocyte. Experiments were performed from 2 to 7 days after injection, and the oocytes were incubated at 18°C. The sterile oocyte incubation solution consisted of 100 mM NaCl, 2 mM KCl, 1.8 mM $CaCl_2$, 1 mM $MgCl_2$, 5 mM HEPES, 10 μM EDTA, and 100 μM DTT.

Effects of Mutations and Probe Labeling on Channel Function

The oocytes were incubated in a depolarizing solution containing 5 μM of the fluorescent probe tetramethylrhodamine-5-maleimide (Mannuzzu et al., 1996) at 18°C for 40 min. Titration of oocyte labeling indicated that for all four constructs, saturation of labeling was achieved by 30 min (data not shown). Because the putative transmembrane topology of hSkM1 contains a number of cysteines that could be available extracellularly, it was first determined whether these cysteines would be labeled by an extrinsic fluorescent probe. To test this, wild-type hSkM1 was expressed in *Xenopus* oocytes, and two groups of oocytes were stained: oocytes expressing the channel and uninjected oocytes. The fluorescence intensity of uninjected, stained oocytes was 994.7 ± 56.8 (arbitrary units ± SEM), whereas the fluorescence intensity of hSkM1-expressing, stained oocytes was 958.8 ± 87.5. Thus, there was no detectable increase in labeling due to expression of wild-type hSkM1. In addition, there was no detectable voltage-dependent change of fluorescence in fluorescently labeled oocytes expressing wild-type hSkM1 (data not shown).

To examine the effects of the cysteine substitutions and probe labeling, the characteristics of the activation and inactivation curves were compared between the wild-type channel and each of the different mutations after probe labeling. The saturation of labeling experiments indicates that with our labeling protocol, the perturbation of function by probe in our experiments is complete. The $t_{1/2}$ to peak current and time constants of inactivation are shown in Table 1. Although the inactivation characteristics of the domain IV construct are notably different, the characteristics of the fluorescence were compared with the ionic currents of the same construct.

Acknowledgments

This work was supported by National Institutes of Health grant GM-30376 and the Hagiwara Chair funds (F. B.), National Institutes of Health grant NS-29204 and the Muscular Dystrophy Association (P. R. and E. F.), and National Institutes of Health grant NS-32387 (A. G.). A. C. is supported by the UCLA Medical Scientist Training Program (GM-08042) and a National Research Service Award from the National Institute of Mental Health (MH-12087). We would like to thank Dr. Ramon Latorre for comments on the manuscript.

Received September 22, 1998; revised November 19, 1998.

References

Aggarwal, S.K., and MacKinnon, R. (1996). Contribution of the S4 segment to gating charge in the *Shaker* K^+ Channel. Neuron *16*, 1169–1177.

Armstrong, C.M., and Bezanilla, F. (1973). Currents related to movement of the gating particles of sodium channels. Nature *242*, 459–461.

Armstrong, C.M., and Bezanilla, F. (1977). Inactivation of the sodium channel. II. Gating current experiments. J. Gen. Physiol. *70*, 567–590.

Armstrong, C.M., and Gilly, W.F. (1979). Fast and slow steps in the activation of sodium channels. J. Gen. Physiol. *74*, 691–711.

Baker, O.S., Larsson, H.P., Mannuzzu, L.M., and Isacoff, E.Y. (1998). Three transmembrane conformations and sequence-dependent displacement of the S4 domain in Shaker K^+ channel gating. Neuron *20*, 1283–1294.

Cha, A., and Bezanilla, F. (1997). Characterizing voltage-dependent conformational changes in the *Shaker* K^+ channel with fluorescence. Neuron *19*, 1127–1140.

Cha, A., and Bezanilla, F. (1998). Structural implications of fluorescence quenching in the *Shaker* K^+ channel. J. Gen. Physiol. *112*, 391–408.

Chahine, M., George, A.L., Jr., Zhou, M., Ji, S., Sun, W., Barchi, R.L., and Horn, R. (1994). Sodium channel mutations in paramyotonia congenita uncouple inactivation from activation. Neuron *12*, 281–294.

Chen, L.Q., Santarelli, V., Horn, R., and Kallen, R.G. (1996). A unique role for the S4 segment of domain 4 in the inactivation of sodium channels. J. Gen. Physiol. *108*, 549–556.

Greenblatt, R.E., Blatt, Y., and Montal, M. (1985). The structure of the voltage-sensitive sodium channel. FEBS Lett. *193*, 125–134.

Ho, H.N., Hunt, H.D., Morton, R.M., Pullen, J.K., and Pease, L.R. (1989). Site-directed mutagenesis by overlap extension using the polymerase chain reaction. Gene *77*, 51–59.

Hodgkin, A.L., and Huxley, A.F. (1952). A quantitative description of membrane current and its application to conduction and excitation in nerve. J. Physiol. *117*, 500–544.

Horn, R., and Vandenberg, C. (1984). Statistical properties of single sodium channels. J. Gen. Physiol. *84*, 505–534.

Kontis, K.J., and Goldin, A.L. (1997). Sodium channel inactivation is altered by substitution of voltage sensor positive charges. J. Gen. Physiol. *110*, 403–413.

Kontis, K.J., Rounaghi, A., and Goldin, A.L. (1997). Sodium channel activation gating is affected by substitutions of voltage sensor positive charges in all four domains. J. Gen. Physiol. *110*, 391–401.

Kosower, E.M. (1985). A structural and dynamic molecular model for the sodium channel of *Electrophorus electricus*. FEBS Lett. *182*, 234–242.

Kuo, C.-C., and Bean, B. (1994). Na^+ channels must deactivate to recover from inactivation. Neuron *12*, 819–829.

Larsson, H.P., Baker, O.S., Dhillon, D.S., and Isacoff, E.Y. (1996). Transmembrane movement of the *Shaker* K^+ channel S4. Neuron *16*, 387–397.

Liu, Y., Jurman, M.E., and Yellen, G. (1996). Dynamic rearrangement of the outer mouth of a K^+ channel during gating. Neuron *16*, 859–867.

Mannuzzu, L.M., Moronne, M.M., and Isacoff, E.Y. (1996). Direct physical measure of conformational rearrangement underlying potassium channel gating. Science *271*, 213–216.

McPhee, J.C., Ragsdale, D.S., Scheuer, T., and Catterall, W.A. (1994). A mutation in segment IVS6 disrupts fast inactivation of sodium channels. Proc. Natl. Acad. Sci. USA *91*, 12346–12350.

McPhee, J.C., Ragsdale, D.S., Scheuer, T., and Catterall, W.A. (1995). A critical role for transmembrane segment IVS6 of the sodium channel alpha subunit in fast inactivation. J. Biol. Chem. *270*, 12025–12034.

McPhee, J.C., Ragsdale, D.S., Scheuer, T., and Catterall, W.A. (1998). A critical role for the S4–S5 intracellular loop in domain IV of the sodium channel alpha-subunit in fast inactivation. J. Biol. Chem. *273*, 1121–1129.

Mitrovic, N., George, A.L., Jr., and Horn, R. (1998). Independent versus coupled inactivation in sodium channels. Role of the domain 2 S4 segment. J. Gen. Physiol. *111*, 451–462.

Noda, M., Shimizu, S., Tanabe, T., Takai, T., Kayano, T., Ikeda, T., Takahashi, T., Nakayama, H., Kanaoka, Y., Minamino, N., Kangawa, et al. (1984). Primary structure of *Electrophorus electricus* sodium channel deduced from cDNA sequence. Nature *312*, 121–127.

Noda, M., Ikeda, T., Kayano, T., Suzuki, H., Takeshima, H., Kurasaki, M., Takahashi, H., and Numa, S. (1986). Existence of distinct sodium channel messenger RNAs in rat brain. Nature *320*, 188–192.

Patlak, J. (1991). Molecular kinetics of voltage-dependent Na^+ channels. Physiol. Rev. *71*, 1047–1080.

Perozo, E., Santacruz-Toloza, L., Stefani, E., Bezanilla, F., and Papazian, D.M. (1994). S4 mutations alter gating currents of Shaker K channels. Biophys. J. *66*, 345–354.

Seoh, S.A., Sigg, D., Papazian, D.M., and Bezanilla, F. (1996). Voltage-sensing residues in the S2 and S4 segments of the *Shaker* K^+ channel. Neuron *16*, 1159–1167.

Shao, X., and Papazian, D.M. (1993). S4 Mutations alter the single-channel gating kinetics of *Shaker* K^+ channels. Neuron *11*, 343–352.

Smith, M.R., and Goldin, A.L. (1997). Interaction between the sodium channel inactivation linker and domain III S4–S5. Biophys. J. *73*, 1885–1895.

Stefani, E., Toro, L., Perozo, E., and Bezanilla, F. (1994). Gating of Shaker K^+ channels: I. Ionic and gating currents. Biophys. J. *66*, 996–1010.

Stimers, J.R., Bezanilla, F., and Taylor, R.E. (1985). Sodium channel activation in the squid giant axon. Steady state-properties. J. Gen. Physiol. *85*, 65–82.

Stühmer, W., Conti, F., Suzuki, H., Wang, X.D., Noda, M., Yahagi, N., Kubo, H., and Numa, S. (1989). Structural parts involved in activation and inactivation of the sodium channel. Nature *339*, 597–603.

Tempel, B.L., Papazian, D.M., Schwarz, T.L., Jan, Y.L., and Jan, L.Y. (1987). Sequence of a probable potassium channel component encoded at *Shaker* locus of *Drosophila*. Science *237*, 770–775.

Vandenberg, C.A., and Bezanilla, F. (1991). A sodium channel gating model based on single channel, macroscopic ionic, and gating currents in the squid giant axon. Biophys. J. *60*, 1511–1533.

Vassilev, P.M., Scheuer, T., and Catterall, W.A. (1988). Identification of an intracellular peptide segment involved in sodium channel inactivation. Science *241*, 1658–1661.

West, J.W., Patton, D.E., Scheuer, T., Wang, Y., Goldin, A.L., and Catterall, W.A. (1992). A cluster of hydrophobic amino acid residues required for fast Na(+)-channel inactivation. Proc. Natl. Acad. Sci. USA *89*, 10910–10914.

Yang, N., and Horn, R. (1995). Evidence for voltage-dependent S4 movement in sodium channels. Neuron *15*, 213–218.